JCI The Journal of Clinical Investigation

Innate immune cell activation by adjuvant AS01 in human lymph node explants is age-independent

Vicki V. Stylianou, … , Kerrie J. Sandgren, Anthony L. Cunningham

J Clin Invest. 2024. https://doi.org/10.1172/JCI174144.

Research In-Press Preview Immunology Vaccines

Graphical abstract

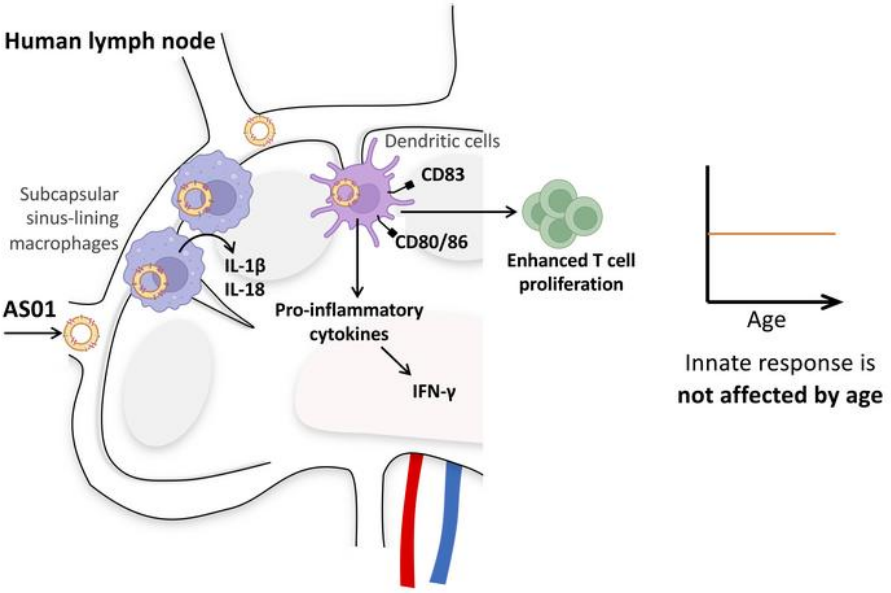

Title: Innate immune cell activation by adjuvant AS01 in human lymph node explants is age-independent.

Authors: Vicki V. Stylianou[1,2], Kirstie M. Bertram[1,2], Van Anh Vo[1,2], Elizabeth B. Dunn[1,2], Heeva Baharlou[1,2], Darcii Terre[1,2], James Elhindi[3], Elisabeth Elder[2,4], James French[2,4], Farid Meybodi[2,4], Stéphane T. Temmerman[5], Arnaud M. Didierlaurent[6], Margherita Coccia[5], Kerrie J. Sandgren*[1,2], Anthony L. Cunningham*†[1,2]

Affiliations:

[1]Centre for Virus Research, The Westmead Institute for Medical Research; Westmead, Australia.

[2]Sydney Medical School, Faculty of Medicine and Health, The University of Sydney; Sydney, Australia.

[3]Research and Education Network, Western Sydney Local Health District; Westmead, Australia.

[4]The Westmead Breast Cancer Institute; Westmead, Australia.

[5]GSK; Rixensart, Belgium.

[6]Center of Vaccinology, Department of Pathology and Immunology, Faculty of Medicine, University of Geneva; Geneva, Switzerland.

*These senior authors contributed equally to this work.

†Corresponding author. Email: tony.cunningham@sydney.edu.au

Conflicts of interest: S.T. and M.C. are employees, own shares and are listed as inventor on a patent owned by the GSK group of companies. A.L.C. received consultancies for GSK and honoraria are paid to their institution for research purposes.

Abstract:

Vaccine adjuvants are thought to work by stimulating innate immunity in the draining lymph node (LN), although this has not been proven in humans. To bridge data obtained in animals to humans, we have developed an in situ human LN explant model to investigate how adjuvants initiate immunity. Slices of explanted LNs were exposed to vaccine adjuvants and revealed responses that were not detectable in LN cell suspensions. We used this model to compare the liposome-based AS01 with its components MPL and QS-21, and TLR ligands. Liposomes were predominantly taken up by subcapsular sinus-lining macrophages, monocytes and dendritic cells. AS01 induced dendritic cell maturation and a strong pro-inflammatory cytokine response in intact LN slices but not in dissociated cell cultures, in contrast to R848. This suggests the onset of the immune response to AS01 requires a coordinated activation of LN cells in time and space. Consistent with the robust immune response observed in older adults with AS01-adjuvanted vaccines, the AS01 response in human LNs was independent of age, unlike R848. This human LN explant model is a valuable tool for studying the mechanism of action of adjuvants in humans and for screening new formulations to streamline vaccine development.

Main Text:

INTRODUCTION

Incorporation of adjuvants into subunit vaccines has markedly increased the long-term immunogenicity and efficacy of these vaccines, particularly in ageing and immune compromised populations. An excellent example is the Recombinant Zoster Vaccine, (Shingrix™, GSK) consisting of recombinant varicella zoster virus glycoprotein E (gE) and the adjuvant system $AS01_B$, with high efficacy in all age groups, including those over 80 years of age (YOA), for at least ten years (1-3). Phase I/II studies showed that the absence of AS01 reduced gE-specific CD4 T cell responses >10 fold in those >70 YOA (4). AS01 consists of a TLR4 agonist, monophosphoryl lipid A (MPL), and the saponin QS-21 formulated in liposomes. The immunostimulants in AS01 act synergistically in mouse models to enhance CD4 T cell responses (5). However, the Recombinant Zoster Vaccine, as shown for other adjuvanted vaccines, presents an increased incidence of local and systemic symptoms occurring shortly after vaccination: 9-11% of recipients experience reactions that prevent daily life activities although these only last for 2 to 3 days (6). However, such reactogenicity is not correlated with immunogenicity (7), suggesting that adjuvants can be modified or developed to retain immunogenicity but with lower reactogenicity.

In order to achieve this, the exact mechanism of action in human subjects needs to be elucidated. For AS01, extensive studies have been conducted in mouse models, showing the rapid transit of AS01 and associated antigens to lymph nodes (LNs) where the onset of the immune response occurs (8). There the immune stimulants are taken up by sinus-lining macrophages, stimulating caspase-1 activation and IL-18 production. Early activation of macrophages initiates a cascade of immune responses including an early burst of interferon gamma (IFN-γ) from natural killer (NK) and $CD8^+$ T cells in an IL-18 and IL-12 dependent manner. This culminates in dendritic cell (DC) activation and presentation of antigen to T and

67 B cells, measured by a marked increase in antigen-specific antibody and polyfunctional $CD4^+$
68 T cells (8-11). Some of these events have been confirmed in non-human primate LNs and
69 human blood (11, 12). However, there are many differences between human and murine
70 immune processes, including in LN (13, 14) and findings in mice should be validated in
71 humans.

72 Therefore, we have developed an in situ human LN explant model to study the mechanism of
73 action of vaccine adjuvants, including AS01, for which abundant data exist in animal models.
74 We found that liposomes of similar composition to AS01 were preferentially taken up by
75 $CD169^+$ sinus-lining macrophages and DCs. AS01 induced maturation of DCs and the
76 production of an array of pro-inflammatory cytokines, including IL-1β, IL-18 and IFN-γ, in
77 intact LN slices but not when LN cells were dissociated from tissue. DCs from AS01 exposed
78 LNs also had an enhanced capacity for naïve T cell stimulation. Unlike the LN response to
79 other adjuvants, the response to AS01 was relatively independent of the adult LN donor's age
80 which may underly the remarkable efficacy of AS01-formulated vaccines in older adults (1,
81 15).

82

83

RESULTS

Human lymph node explant model

To study the mechanisms of action of adjuvants in situ in human tissue, we developed a human LN explant model. Uninvaded human axillary LNs were obtained from female breast cancer patients who were clinically node negative but undergoing sentinel node biopsies. Informed consent was obtained for the removal of an additional LN for this study. Donors were aged between 30 and 96 YOA. 53% were ≥ 60 YOA (Supplemental Figure 1). Longitudinal slices of whole human LNs, approximately 2 mm thick, were cultured on gel foam to provide hydration and structural support, which promoted cell viability (Figure 1A).

We used a high-parameter flow cytometry panel to detect all subsets of myeloid cells, which include resident DC subsets including conventional type 1 and 2 DCs (cDC1, cDC2) and plasmacytoid DCs (pDC), sinus-lining and medullary macrophages (SM and MM) and monocytes (mono), as well as NK, NK-T, B and T cells (Figure 1B). Migratory skin-derived DCs ($CD11c^{+}CD1a^{+}Langerin^{+/-}$) that were present in the LN at the time of excision were also detected. First, we assessed the viability of different cell populations in LN explant cultures by flow cytometry. T, B and NK cells survived for 48-72 h but viability of the DCs and macrophages declined in the LN over 24 h culture (Figure 1C). Macrophages in particular exhibited reduced numbers after explant culture, rather than appearing more strongly stained with the viability marker, indicating that they were lysing (Supplemental Figure 2A). Importantly, the viability of cells in LN slices cultured for 24 h was similar whether or not the cultures were stimulated with adjuvant AS01. AS01 was well tolerated up to a concentration of 25 μg/mL in situ and in vitro but higher concentrations decreased viability (Supplemental Figure 2). Furthermore, the viability of total dissociated LN cells, which is comprised of > 98% lymphocytes, cultured in vitro for 24 h (72.9 ± 17.0%, mean ± SD; Supplemental Figure 2C), was only slightly better than the viability of the lymphocytes cultured in LN slices (T cells 69.7

± 7.6%, B cells 68.8 ± 11.8%; Figure 1C). As such, we limited explant cultures to 24 h and included mock treated controls to account for any effects produced by dying cells.

Next, we compared the immune cell constitution of LNs from young (≤50 YOA, n = 12) and older individuals (>65 YOA, n = 22) in fresh, uncultured LNs. LNs from young or old donors were remarkably similar. T and B cells represented the bulk of cells, with CD3-CD19-HLA-DR^+ antigen presenting cells representing 1.79 ± 1.16% in young and 1.43 ± 0.84% in old LNs (mean ± SD) (Figure 1D). The constitution of this HLA-DR^+ population was also remarkably similar between the two age groups with no significant differences in the cell subset proportions (Figure 1E).

$CD169^+$ sinus-lining macrophages preferentially take up AS01-like liposomes

To assess the effects of adjuvant on LN explants, adjuvant treatments were applied via two routes (Figure 1A): a cloning cylinder glued to the capsule of the LN allowed the adjuvant to enter the LN probably via the afferent lymphatic vessels on the LN surface, as occurs in vivo or possibly penetrating through the capsule directly. Alternatively, the cut face of the LN was exposed directly by placing it on gel foam soaked in adjuvant-containing culture medium ('bathing'; Figure 1A) and this allowed for maximum exposure of LN immune cells, which yielded stronger immune responses. To model the uptake of AS01 in situ in LNs, we used liposomes of equivalent composition and similar size, without MPL and QS-21 but incorporating the lipophilic fluorescent dye DiO or DiD. Slices of human LNs were exposed in situ to labeled liposomes via both the bathing and cylinder application methods for 30 min to 24 h to determine the degree of liposome uptake for each immune cell subset by flow cytometry (Figure 2A). Immunofluorescence microscopy confirmed that liposomes penetrated the LN slice within 30 minutes via bathing (Figure 2B) and the degree of penetration increased

over 24 h (Supplemental Figure 3A). Correspondingly, uptake of liposomes by each cell type increased over 24 h (Figure 2C). For all subsets, a larger percentage of cells were exposed to the liposomes via bathing compared to cylinder application resulting in a higher degree of uptake, as shown by the percentage of cells that were liposome positive (Figure 2D, Supplemental Figure 3B). However, the distribution of liposome uptake across subsets was proportional (Figure 2E-F, Supplemental Figure 3C), with a strong correlation between the two exposure routes (Supplemental Figure 3D), indicating that the liposomes penetrated the LN effectively via both methods and the bathed route did not introduce a bias on liposome uptake. We therefore conducted all experiments using the bathing exposure method as it a) increased exposure of the cells to the liposomes and therefore presumably the adjuvant and b) did not result in exposure of any cells that would not normally encounter the adjuvant when exposed via the physiological route simulated by the cloning cylinder.

The $CD169^+$ SMs, found both in the medullary sinuses and the subcapsular sinus had the highest capacity for liposome uptake at the single cell level (Figure 2D), likely due to the superficial position of the subcapsular SMs, lining the large peripheral sinuses of the LN (Figure 2G) and also their innate capacity for particle uptake. The accumulation of liposomes in the cytoplasm of $CD169^+$ subcapsular SMs was confirmed by microscopy (Figure 2H). The remaining macrophage and monocyte subsets also had a relatively high capacity for liposome uptake, especially $CD14^+$ monocyte-derived DCs (MDDCs). Of the DC populations, cDC2s were more efficient at liposome uptake than cDC1s, with migratory dermal cDC2s being better than resident cDC2s (Figure 2D). pDCs took up very little liposome. This hierarchy is consistent with the generally documented phagocytic capacity of these cells (16). These results are also consistent with reports in mice highlighting the role of subcapsular SMs in the initial uptake of AS01 and the critical role of subcapsular SMs and cDC2s in the initiation of the immune response (10, 11).

Liposomes were poorly taken up by lymphocytes, with only a modest increase in fluorescence over 24 h (Figure 2C) and was likely only surface associated. Of the total liposome positive cells, HLA-DR$^+$ antigen presenting cells (APCs) were over-represented, at 8.93 ± 7.03% (mean ± SD, n=5), despite representing only 1.55 ± 0.90% (mean ± SD, n=49) of live CD45$^+$ cells in the LN (Figure 2E, F). Myeloid cells, particularly SMs, also preferentially took up liposomes compared to their proportion of the total cell population (Figure 2E, F).

AS01 induces maturation of dendritic cells, but only in intact human lymph nodes

A key property of an adjuvant is the capacity to enhance activation of APCs, inducing their upregulation of co-stimulatory molecules (CD80, 83, 86) which allow them to stimulate T cell proliferation. We assessed whether AS01, its component MPL and QS-21, or other Toll-like receptor (TLR) ligand adjuvants – R848 (TLR7/8) and Pam2Cys (TLR2) – induced maturation of LN myeloid cells and activation of NK cells and lymphocytes. Initially, to clarify the direct effect of AS01 on immune cells, cells were mechanically dissociated from LN tissue and stimulated as a mixed population with AS01 in vitro for 24 h. MPL and R848 were included as comparators. AS01 induced no or very weak upregulation of the maturation markers CD80 and CD86 on dissociated DCs compared to donor matched control samples. AS01 also did not activate lymphocytes and NK cells, measured by CD69 upregulation (Supplemental Figure 4). MPL was similarly non-stimulatory in vitro at an equivalent concentration to the MPL component of AS01. In contrast, R848 was potent at inducing upregulation of CD86 on macrophages, cDC2s (CD14$^-$CD11c$^+$ cells) and pDCs, and in 4/6 cDC1 donors, as well as CD69 upregulation on NK, NK-T, T and B cells (Supplemental Figure 4).

In contrast to the in vitro results, AS01 did induce maturation of cDCs when intact LN slices were exposed in situ for 24 h. We observed significant upregulation of CD83 and CD86 on

cDC1s and CD80 and CD83 on cDC2s (Figure 3A). CD86 and CD83 were significantly upregulated when resident cDC2s were analysed by subsets, including langerin^{+} and langerin^{-} subsets (Supplemental Figure 5). In some donors, rare DC subsets, such as cDC1s, could not be detected. Higher concentrations of AS01 tended to reduce cell viability (Supplemental Figure 2D) as well as the maturation response (Supplemental Figure 5B). Unlike AS01, the other stimuli QS-21, MPL, R848 and Pam2Cys did not consistently induce maturation of cDCs in situ, although R848 did mature pDCs, increasing their expression of CD86 (Figure 3A), and activated both NK and B cells (Figure 3B). The results of these two experiments show that AS01 induces maturation of cDCs but only when the LN structure is intact. This suggests that rather than directly activating DCs, AS01 induces this effect via an amplifying immune cascade that requires not only the presence of multiple cell types, but critically, also the native structural organisation of the LN. It also shows that lymphocytes are not directly activated by AS01. Conversely R848 was more effective in directly activating TLR7/8-expressing cells in vitro than in the tissue, while QS-21, MPL and Pam2Cys did not induce cellular maturation or activation by themselves.

AS01 induces pro-inflammatory cytokines, but only in intact human lymph nodes

We assessed the cumulative production of pro-inflammatory cytokines in response to AS01, R848 and MPL, when dissociated LN cells were exposed in vitro and all five adjuvants when whole LN slices were exposed in situ for 24 h. As with maturation, no pro-inflammatory cytokines could be consistently detected after AS01 stimulation of the total dissociated cell population in vitro (Supplemental Figure 6). IL-1β was detected in 4/10 donors. Conversely, and consistent with its in vitro effect on maturation, R848 did induce inflammatory cytokines IFN-α, IL-1β, -18, -6, -8, and TNF as well as anti-inflammatory IL-10 and showed a trend for

the induction of IFN-γ in 5/8 donors. MPL was less inflammatory, significantly inducing IL-6, and -8 and inducing an increase in IL-1β and -18 in 5/7 donors (Supplemental Figure 6).

Although AS01 was rather inert in isolated cells, as with myeloid cell activation, we saw a much greater immune response in the more physiological in situ exposure model in terms of pro-inflammatory cytokine induction. We therefore focused on the in situ model and included QS-21 formulated in liposomes and Pam2Cys with the other stimuli. In situ, AS01 induced a range of pro-inflammatory cytokines, including IL-1β, -18, -6, -23, as well as TNF and IFN-γ (Figure 4A). There was a trend towards increased IL-12p70 (p=0.062) but IL-17A, IL-10 and IFN-α were not detected in response to AS01. Higher concentrations of AS01 did not increase the level of cytokine production (data not shown), consistent with the previously demonstrated decreased viability and maturation. MPL was again less inflammatory, only inducing IL-1β and downregulating IL-10. Cytokine induction by MPL was also compared to MPL formulated in liposomes and found to be comparable (Supplemental Figure 7). QS-21 in liposomes induced a similar cytokine profile to AS01, with the exception of TNF and IL-12p70. R848 induced an even broader range of cytokines in situ than in vitro, adding IL-12p70, IL-23, and clear induction of IFN-γ to its in vitro profile, although IL-18 was not significantly induced in situ. Pam2Cys was tested in situ and although it did not induce cellular maturation or activation it did induce a broad inflammatory response with IL-1β, -6, -8, TNF and IFN-γ detected (Figure 4A). Furthermore, when a time course was performed, the induction of these cytokines was dynamic over 24 h. For example, IL-1β and IL-18 were induced within 8 h and IFN-γ did not appear until 24 h following AS01 stimulation (Supplemental Figure 8).

To summarise, in keeping with the maturation data, apart from IL-1β in some dissociated cell donors, AS01 only induced pro-inflammatory cytokines in intact LN tissue, again suggesting the requirement of the LN structure for the transmission of signals to multiple cell types upon

exposure to AS01. QS-21 induced a similar pro-inflammatory cytokine response to AS01. At the concentrations tested, R848 was more immunostimulatory, activating several cell subsets directly, while MPL and Pam2Cys were less immunostimulatory with moderate activation of the immune system both in vitro and in situ.

In mice, it has been shown that AS01 triggers an immune cascade, beginning with the activation of subcapsular SMs that produce IL-18. In synergy with IL-12, IL-18 rapidly enhances early IFN-γ production from NK and $CD8^+$ T cells (10, 11). The production of IL-18 is linked to pyroptosis of the cell (17). In this study, after in situ AS01 exposure, the frequency of $CD14^+$ cells, including macrophages, was significantly reduced (Figure 4B) and IL-18 production inversely correlated with the size of the $CD14^+$ population (Pearson's correlations r=-0.679, p=0.005) (Figure 4C). Samples that had a strong upregulation of IL-18 in the supernatant, had very depleted macrophage populations, with very few $CD14^+$ cells and no discernible $CD169^+$ SM population. Correlation of IL-18 production with the SM population was therefore weaker (r=-0.641, p=0.010). Samples that had weak or no induction of IL-18 had much more robust populations, still smaller than the original population when the tissue was fresh, but distinct $CD14^+$ and $CD169^+$ populations remained. Therefore, it is likely that macrophages produce IL-18 in response to AS01 in situ, although they are dying in the process, as seen for QS-21 in mice (10). Increased IL-18 production however did not correlate with increased DC maturation (data not shown).

To confirm the discrepancy between our in vitro and in situ results, we directly assessed a range of cytokines by intracellular cytokine staining (ICS) in dissociated human LN cells in vitro. IL-18 production is difficult to detect by ICS due to the induction of pyroptosis, as mentioned above. IL-1β, clearly induced in situ by AS01 in human LNs although only detected in very low amounts in mice upon AS01 administration (8), is produced by a common activation pathway to IL-18 but we could detect this by ICS. R848, included as a comparator, induced IL-

255 1β production by $CD14^+$ cells, which included macrophages, and IL-12/23p40 production by
256 $CD1c^+$ cDC2s. NK and T cells could produce IFN-γ in response to PMA/ionomycin stimulation
257 (Figure 5). In contrast, AS01 induced IL-1β in macrophages from 5/5 donors but did not induce
258 IL-12/23p40 in cDCs or IFN-γ in NK or T cells from any donors (Figure 5). These results were
259 the same regardless of whether brefeldin A was added early (2 h into the culture, potentially
260 blocking the early release of cytokines and their downstream effects such as IFN-γ induction)
261 or late (8-12 h into the culture, allowing more time for the full cytokine cascade before its
262 addition) and therefore the combined data is shown (Figure 5E).

263 The induction of IL-1β and IL-18 in situ and at least IL-1β in vitro, is consistent with the early
264 AS01/QS-21 cytokine cascade shown in mice (8, 10, 11, 18), however, in humans when cells
265 are dissociated from the LN, the downstream parts of the AS01 cytokine cascade are lost,
266 highlighting an important role for this LN explant system in preserving the cell-cell contact
267 required for the native immune responses.

268

269 **Age did not influence basal levels of dendritic cell maturation and cytokine release in the**
270 **lymph node but did influence the dendritic cell response to adjuvants**

271 Ageing results in disturbances in the structure of LNs, disorganization of the internal zones and
272 impaired intercellular interactions and cytokine responses (19, 20). Together with a reduced
273 thymic output of naïve T cells, these changes result in impaired immune responses to pathogens
274 and vaccines.

275 In terms of functional effects, we did not observe a difference in the basal expression of co-
276 stimulatory molecules CD83 or CD86 on cDC1, cDC2 or pDCs from older (≥60 YOA)
277 compared to younger adults (<60 YOA) (Figure 6A). Furthermore, cDC2s from younger

donors upregulated CD83 more than older donors in response to AS01 but otherwise there was no difference in DC capacity to mature in response to AS01 or R848 in situ (Figure 6B).

Whilst increased circulating levels of TNF, IL-1β and IL-6 have been reported in ageing adults >65 YOA compared to young adults <30 YOA (21), we did not observe this in LNs in our cohort in unstimulated LN slices. Initially, in a univariate analysis, we found no difference in the basal level of these or other pro-inflammatory cytokines in the supernatants of cultured LNs from older or younger donors (Figure 7A). As with maturation, we also did not find a significant difference in the capacity of older LNs to respond with pro-inflammatory cytokines to any of the adjuvants when comparing the median fold-change (Figure 7B, Supplemental Figure 9). To further investigate the impact of ageing, we used a robust general estimating equation (GEE model) to cluster readings by donor, considering age as a continuous variable. Here, an interaction between age and adjuvant was identified for IFN-γ and IL-18 (Figure 7C, Table I), indicating that adjuvants have different effects on cytokine production depending on the age of the subjects. A natural increase in IFN-γ production and IL-18 production was observed with age in mock stimulated cultures, consistent with inflammaging (22) and previous reports (23, 24), e.g. each YOA confers an additional immune response of 0.027 log-IFN-γ units (Table I). IFN-γ production in response to R848 strongly and significantly increased with age, although the opposite has been reported in blood (21). IFN-γ production in response to AS01 only increased slightly, and was not significantly different to the natural increase observed with age alone. These two adjuvants differed from MPL and Pam2Cys, where there was no age relationship for the IFN-γ response. The IL-18 response to R848 and Pam2Cys increased with age at a similar rate but only the R848 response was significantly greater than the natural increase. The response to MPL also only increased in line with the natural increase. In contrast, the age-related increase in IL-18 in response to AS01 was slower than the natural incline with age although their confidence intervals slightly overlapped (Table I). Thus, we

observed differential responses to TLR ligands with age but a consistent AS01-induced pro-inflammatory response was maintained in LNs from younger and older adults.

AS01 enhances the capacity of dendritic cells for stimulating naïve CD4+ T cells

To explore the functional implications of the innate immune activation induced by AS01, we assessed DCs primed in AS01-exposed LN slices for their capacity to induce proliferation of heterologous naive CD4+ T cells. The latter have a higher threshold for activation than memory T cells and their stimulation is important for both initial and booster vaccine doses (25, 26). AS01 primed DCs with enhanced antigen presentation capacity compared to mock stimulated LNs (Figure 8A). The degree of proliferation correlated with the AS01-induced maturation (CD83 expression) of a subset of DCs, langerin+ cDC2s, with a trend towards correlation in total DCs (Figure 8B; Supplemental Figure 10).

DISCUSSION:

Predictive pre-clinical models to define the immunogenicity and mechanisms of action of vaccines and adjuvants in humans could be instrumental in the iterative development of new vaccines. Here we have demonstrated the utility of a human LN explant model for investigating in situ innate immune responses to vaccine adjuvants. In this model, whole tissue slices were used to preserve the complex internal structure of the LN including the capsule, at a thickness designed to maximise representation of all compartments and the number of rare APC subsets that may be lost in small tissue blocks or thin slices. Cascading immune responses were preserved that were otherwise lost in dissociated cells, demonstrating the physiological relevance of the model and the importance of maintaining the spatial organization of cells and extracellular matrix structures within the organ. This model can be used as an additional tool to in vivo mouse and non-human primate models for testing mechanisms of action of existing and novel vaccines and adjuvants, and their immunostimulatory properties at the very site where they work in vivo, after intramuscular injection. With this human model, we investigated the innate immune response to AS01 spanning the initiating events through to the interface of innate and adaptive immunity. We describe the key LN cells that are targeted and stimulated by AS01 and demonstrate the functional consequence of this. Liposomes with similar composition to those found in AS01 were preferentially taken up by subcapsular SMs and DCs, with SMs likely being the initial cells to respond. AS01 induced maturation of multiple subsets of DCs, as well as the production of pro-inflammatory cytokines from multiple cell types, in in situ exposed LN slices but not in dissociated LN cell cultures. This led to DCs with enhanced potency for stimulating naïve CD4+ T cell proliferation. The age of the adult LN donor did not influence the production of cytokines in response to AS01, unlike other adjuvants. This may be one factor underlying the efficacy of AS01-formulated vaccines, e.g. for herpes zoster and respiratory syncytial virus in older adults (1, 15).

We have made several findings that demonstrate there are strong similarities between the mode of action of AS01 in mice and humans. 1. Pattern of uptake in LNs, primarily by $CD169^+$ subcapsular SMs but also DCs; 2. Activation of APCs - macrophages and DC; 3. Initiation of a cytokine cascade that culminates in the early production of IFN-γ. The latter is likely produced by NK or CD8+ T cells.

Particles approximately 10 – 100 nm in size can flow freely to the LN via the lymphatics (27) and AS01 is approximately 100 nm (28). Indeed in mice, QS-21 in liposomes drains to the lymph node via the afferent lymphatics within 30 minutes of administration and is taken up by $CD169^+$ macrophages that line the sinuses of the LN, including the subcapsular sinus, that are ideally positioned to sample lymph-borne antigen (10). These subcapsular SMs play an important role in transferring captured antigen to and activating B cells and produce an array of cytokines to coordinate multiple LN resident immune cells (29). The uptake of our empty liposomes by subcapsular SMs and also DCs is consistent with this and the pattern was the same whether liposomes were applied by a cloning cylinder to the external surface, or by bathing the entire cut surface of the explant. The latter may be explained by the size of the liposomes. Particles > 10 nm are too large to flow through the narrow lymphatic conduits to access the paracortex with its T cells and DCs (27), however, they can access the subcapsular SMs, DCs and other cells in the superficial interfollicular cortex via the wider peripheral sinus and limited percolation into the tissue. AS01, being slightly smaller than our empty liposomes, may penetrate deeper into the cortex and paracortex. Thus, the superior liposome uptake by CD169+ subcapsular SMs is likely to be due to a combination of their advantageous location and inherent endocytic capability.

The adjuvanticity of AS01 in mice is in part due to the activation of DCs (8, 30). AS01 activated macrophages and cDCs in situ in the human LN model, inducing upregulation of co-stimulatory molecules. R848, a TLR7/8 ligand, did not mature cDC2s in situ, even though they

367 express TLR8 and they were activated in vitro. R848 did mature pDCs, which express high
368 amounts of TLR7, as well as NK and B cells (both $TLR7^+$). R848, a small molecule immune
369 potentiator, would be able to penetrate the LN thoroughly but may have a stronger affinity for
370 TLR7 than TLR8, or the lack of cDC2 activation may be a dose effect with R848 being diluted
371 in the LN explants.

372 A key cytokine axis in the AS01 response in mice is the IL-18/IL-12-dependent induction of
373 IFN-γ (11). QS-21 has been shown to activate the NLRP3 inflammasome, resulting in IL-1β
374 and IL-18 production (10, 18), although in response to AS01, IL-1β has only been detected at
375 very low levels in mice (8) and whether AS01 activates the inflammasome is still unclear. Our
376 findings in human LNs that AS01 induces IL-1β, IL-18, IL-12 detectable in some donors, and
377 IFN-γ, with different kinetics over 24 hours, supports a similar cytokine cascade in humans
378 that likely begins with inflammasome activation in macrophages and culminates in the
379 production of IFN-γ. Interestingly, QS-21 alone did not induce TNF or IL-12 and the induction
380 of these two cytokines may be a key feature of the interaction between MPL and QS-21 in
381 AS01.

382 As we found, stronger and broader cytokine responses in intact lymphoid tissue slices
383 compared to dissociated cell cultures have also been observed before (31-33). The
384 bioavailability, and therefore potency of an adjuvant used at similar doses should be higher in
385 dissociated cultures than in situ cultures so the phenomenon likely relates to the need for
386 complex cell-cell interactions along the reticulin framework (34, 35) as well as cytokine
387 signaling. 3D cytokine gradients will be established much more effectively when the producing
388 cells are fixed in place or utilizing the LN architecture to move in a deliberate direction, as in
389 intact tissue, rather than floating freely. IFN-γ-producing NK and $CD8^+$ T cells may also need

to be in close proximity to IL-12 and IL-18 production which suggests a compartmentalisation of the AS01 response to the subcapsular region of the LN.

Ageing and immunosenescence have a detrimental effect on vaccine responses, with the efficacy of most vaccines being reduced in people over 65 YOA (36-39). However there were vast differences between Recombinant Zoster Vaccine and the live herpes zoster vaccine, with efficacy decreasing markedly with age for the latter vaccine, especially over time (40). The AS01-adjuvanted Recombinant Zoster Vaccine and the Respiratory Syncytial Virus vaccine have overcome this (1-3, 15) but the reasons why this adjuvant is so effective in immunogenicity and efficacy in older adults are unknown (4, 41). We found the immune constitution of old and young LNs was remarkably similar even with a 15 year age gap buffer. This is consistent with reports that the number and phenotype of circulating DCs is comparable in healthy older adults (42, 43), and young adults, apart from the frail elderly (44). This similarity implies that any differences in adjuvant immune responses observed between young and old donors would likely be due to differences in the functional capacity or interactions of immune cell subsets or the structure of the LN between young and old, rather than differences in the frequency of individual cell populations. In the clinical trials of Recombinant Zoster Vaccine there were no gender specific effects identified at any age, including those >70 YOA (45). Therefore, even though only female lymph nodes were tested in this study, in this setting the effect of age is clearly more important than gender.

Although inflammaging, the age-related increase in inflammation, is characterised by an increase in the circulating levels of pro-inflammatory cytokines IL-1β, IL-6 and TNF and reduced levels of anti-inflammatory cytokines such as IL-10 (46, 47), we did not observe these changes in the LNs from donors older or younger than 60 YOA. The increase in circulating pro-inflammatory cytokines in older adults may be driven by altered gut integrity or microbiota, or adipocytes, which increase with age and are another source of pro-inflammatory

cytokines (48, 49). Our GEE model for testing the effect of age on adjuvant-induced cytokine production was influenced by a paucity of donors at the far ends of the age spectrum as well as the expected wide human donor variability of cytokine production and thus had wide confidence intervals. Nonetheless, IL-18 and IFN-γ pathways were found to be particularly conserved across the adult age spectrum, compared to other adjuvants, which may contribute to the efficacy of AS01 in older adults. This is consistent with a recent report that found no age related differences in response to AS01 in human blood myeloid cells (50) although as peripheral blood mononuclear cells are phenotypically and functionally divergent from LN cells (51) it is important to study both.

Using this in situ culture method for LN slices we have demonstrated a dynamic innate immune response to AS01 over 24 h with cytokines being produced with different kinetics and the activation of DCs with the functional capacity to stimulate naïve CD4+ T cells. T cell proliferation was most closely correlated with maturation of the Lang+ cDC2 subset. Notably cDC2 have been identified in mice as necessary for the induction of adaptive immunity by AS01-containing vaccines and AS01 is associated with potent activation of these cells (30). Also Lang+ cDC2s have a higher intrinsic level of *ICAM1* (CD54) expression than Lang- cDC2 in anogenital mucosa, which is critical for DC:T cell interactions, and are the most efficient at transferring HIV to CD4+ T cells (52), which suggests their particular efficiency for interacting with T cells.

Our model has several limitations. The viability of thick tissue explants is difficult to maintain ex vivo, with deeper parts of the tissue affected by hypoxia and diminished nutrient supply. The duration of viability of myeloid and lymphoid cells after isolation from our cultured 2 mm thick LN slices varied but was consistent with findings in similar models (33, 53, 54) and sufficient to allow determination of their early function in response to various adjuvants. Isolation of the cells from tissue after culture is stressful on the cells and it may be possible to

observe and measure immune responses in situ for longer than 24 h. Smaller tissue blocks have been reported to remain viable for three weeks or more (55) but will often not contain the full gamut of sparsely distributed innate and stromal cells and be mostly composed of lymphocytes. Our model will require modification, such as judicious cytokine support or perfusion, to improve its longevity to allow establishment of germinal centres, which generally takes around 4-5 days. Secondary lymphoid organoids, derived from human tonsil have been described that develop functional germinal centres but the complex structure of the LN including the supporting stromal cells is likely not fully recapitulated and they do not have afferent lymphatics or migratory DCs (56). Mechanisms of action of adjuvants on innate cells may be more suited to study in whole LN slices.

Another important limitation of the model is the removal of the blood and lymph circulation. Peripheral immune cells can no longer enter the LN via the afferent lymphatics or high endothelial venules. In a vaccination setting, antigens and adjuvants can be transported by APCs, including DCs, monocytes, and neutrophils (8, 57, 58) from the site of administration to the draining LN and migrating monocytes and DCs contribute to the cytokine milieu in vivo (30). Our model is suited to studying vaccines and adjuvants that can flow freely to the LN. We also did not take into account soluble plasma-derived mediators in this project.

The value of this human LN model is in testing the mechanism of action of vaccines and adjuvants in a human setting. This pre-clinical model holds the potential for comparisons of immunogenicity between different adjuvants and modifications of existing adjuvants by medicinal chemistry, as well as the comparison of modes of action of different vaccine technologies, such as adjuvanted, live attenuated and mRNA-based vaccines. It provides a benchmark for comparison with other models such as mice, human lymph node aspirates or complex blood/lymphoid derived in vitro models.

METHODS

Sex as a biological variable

Our study exclusively examined female human lymph nodes as males rarely undergo axillary sentinel node biopsies for breast cancer or other causes. Axillary lymph nodes are the draining lymph nodes for vaccines delivered in the upper arm. In the pivotal Recombinant Zoster Vaccine trials there were no gender specific effects found at any age including those >70 years of age (45), therefore we expect our findings to be relevant to both sexes.

Human lymph node explant model

Human axillary LNs were obtained from clinically node negative breast cancer patients who were undergoing sentinel node biopsies and consented to the removal of an additional LN for this study. Additionally, participants had no relevant comorbidities and were not on immunomodulating drugs such as steroids or cytotoxic drugs that could be lymphocytic. The donors ranged from 30 to 96 YOA and the LN size ranged from 3-20 mm in the longest dimension. Data was excluded if LN samples had poor viability and where insufficient myeloid cell numbers were recovered from a sample. This most often occurred in LNs that were excessively damaged by cauterisation during excision. In addition, data would also be excluded from any participants confirmed pathologically to have cancer affected LNs. There were no cases of this in the present study.

Within 60 minutes post-surgery, LNs were collected and trimmed of excess fat under a stereo microscope and cut longitudinally into two or three 2 mm thick by 5-7 mm wide slices. These were cultured in 48 well plates, cut face down, on gelfoam (Pfizer) pre-soaked with culture medium formulated to support DC viability (DCM; RPMI (Lonza) supplemented with 10 μM HEPES, 1 mM sodium pyruvate, 1X non-essential amino acids, 0.05 mM gentamicin (all Gibco, Thermo Fisher Scientific), 50 μM 2-mercaptoethanol and 10% human serum (both

Sigma-Aldrich, Merck), v/v), with or without adjuvant. In some instances, a 6 mm cloning cylinder was sealed to the capsule of the LN slice using surgical glue and the stimulus was applied through this to simulate exposure via the afferent lymphatics. LN slices were cultured for up to 24 h as indicated in individual experiments. Supernatants were collected and cells were either mechanically dissociated for flow cytometry analysis or tissue slices were fixed or frozen for microscopy. Alternatively to the in situ exposure model, cells were dissociated from fresh LN tissue and immediately assessed by flow cytometry or stimulated in vitro at 1 x 10^6 cells/mL with adjuvants for 24 h. The adjuvants used for stimulation were 25 µg/mL AS01, one quarter of the AS01 concentration administered intramuscularly in humans ($AS01_B$), 25 µg/mL MPL formulated in liposomes and 25 µg/mL QS-21 formulated in liposomes (GSK), 25 µg/mL unformulated MPL, 10 µg/mL R848 and 1 µg/mL Pam2Cys (InvivoGen). Unformulated MPL was used throughout. MPL in liposomes was only used in direct comparison with unformulated MPL (Supplemental Figure 7 and S8). 10 mM DiO or DiD-labeled liposomes (DOPC:Cholesterol 54:45 mol/mol, 1/200 dye:lipid; mean diameter 200 nm) were kindly provided by Dr. Harry Al-Wassiti (Monash University, VIC, Australia). For in vitro intracellular cytokine staining (ICS) assays by flow cytometry, cells were stimulated for a total of 24 h at 10 x 10^6 cells/mL with AS01, R848 or 50 ng/mL PMA/1 µg/mL Ionomycin (Sigma-Aldrich (Merck)). 2.5 µg/mL Brefeldin A (BFA, Sigma-Aldrich (Merck)) was added after 2 h or 8-12 h of culture.

Flow Cytometry

Cells were stained with Live/Dead Fixable Viability Stain 700 (BD) for 30 min at 4°C. A panel of surface antibodies was then used to stain cells (2.5 x 10^6 cells/100 µL test), according to standard procedures, in FACSwash (PBS/1% FCS (Sigma-Aldrich (Merck)/5 mM EDTA). Cells were fixed with BD Cytofix prior to acquisition. If intracellular staining was required, cells were permeabilized with BD Cytofix/Cytoperm and stained with antibodies prior to

acquisition. For intracellular cytokine staining assays including BFA, all antibody staining was conducted intracellularly. Cells were acquired on the BD Symphony flow cytometer and data analysed by FlowJo V10.8.1 and GraphPad Prism 9. Antibodies included: from BD: CD11c BUV661 (B-ly6), CD14 BUV737 (M5e2), CD1a BV510 (HI149), CD1c BV650 (F10/21A3), CD3 BUV496 (UCHT1), CD45 BUV805 (HI30), CD56 BUV563 (NCAM16.2), CD69 BV480 (FN50), CD8 FITC (5C3), CD80 FITC (L307.4), CD83 PE (HB15e), CD86 BV786 (2331 (FUN-1)), HLA-DR BUV395 (G46-6), IFN-γ PE-Cy7 (B27); from Biolegend: CD11b BV711 (ICRF44), CD123 PE-Cy5 (6H6), CD16 BV570 (3G8), CD19 BV750 (HIB19), CD68 APC-Cy7 (Y1/82A), XCR1 BV421 (ZET); from Thermo Fisher Scientific: CD13 PerCP ef710 (WM15), CD169 PE-ef610 (7-239), IL-1β PE (CRM56), IL-12/23p40 ef660 (HP40), IL-12/IL-23p40 PE (C8.6); from Miltenyi: Langerin PE-Vio770 (MB22-9F5).

Microscopy Imaging

LN slices stimulated in situ with DiD-labeled liposomes were frozen in OCT. 7 μm sections were fixed with 2% paraformaldehyde (PFA) then blocked and permeabilised with PBS/0.1% saponin/1% BSA/10% normal donkey serum/1% HEPES. Tissue was incubated with primary antibodies CD11c (clone 3.9, Invitrogen) and CD169 (SP216, Merck) for 1 h at 37°C and secondary antibodies donkey anti-mouse AlexaFluor 555 and donkey anti-rabbit AlexaFluor 647 for 30 min at room temperature (RT). The tissue sections were counter stained with DAPI and mounted with ProLong Diamond (Thermo Fisher Scientific). Images were acquired on the Olympus VS-120 Virtual Slide Microscope at 20X and analysed using Fiji.

For imaging mass cytometry (IMC), 5 μm FFPE tissue sections were de-waxed and re-hydrated in xylol for 3 x 5 min, 100% ethanol for 3 x 5 min and 70% ethanol for 5 min then PBS. Antigen retrieval was performed in Dako AR Buffer pH 9.0 at 95°C for 20 min in a Biocare Decloaker NxGen. Slides were blocked with Bloxall (Vector Labs) at RT for 10 minutes then incubated with a metal-conjugated antibody cocktail in TBS-Tris/1% BSA overnight at 4°C. Slides were

washed in PBS/0.1% Triton-X for 2 x 8 mins. This was repeated with PBS. Nuclei were stained with a DNA intercalator for 30 min at RT. Images were acquired on a Hyperion Imaging Mass Cytometer (Standard Biotools).

Cytokine immunoassays

The LEGENDplex bead-based multi-analyte flow assay kit (Human Inflammation Panel 1, Biolegend) was used to detect a panel of 13 human inflammatory cytokines in culture supernatants as per the manufacturers' protocol. IL-6 and IL-8 were measured by ELISA (both Biolegend) as their concentrations exceeded the range of the LEGENDplex assay. For LEGENDplex experiments, plates were acquired on the BD Canto II and data analysed with LEGENDplex Data Analysis Software (Biolegend). For all ELISA assays, absorbance was measured on the SpectraMax iD5 Plate Reader and data analysed using GraphPad Prism v9.20.

T cell alloproliferation assay

Following mock or AS01 treatment of LN slices for 20 h, cells were isolated from the tissue by digestion with 3 mg/mL collagenase type IV (Worthington) with 250 U/mL DNAse (Roche) for 40 min at 37°C. Cells were washed and stained with viability dye FVS700 (BD) and CD3 APC-Vio770, CD19 APC-Vio770, HLA-DR PerCP (all Miltenyi Biotech), CD14 BV480, CD11c BB515, CD1c BV650, CD83 PE (all BD), XCR1 APC, CD123 PE-Cy5 (all Biolegend), and CD169 PE-efluor610 (Thermo Fisher) antibodies. DCs were then sorted on a BD Influx cell sorter (BD Biosciences) by gating on live, CD3-, CD19-, CD14-, autofluorescence-, HLA-DR+ cells. 10 - 15,000 DCs were co-cultured at a ratio of 1:2.5 with CellTrace Violet (Thermo Fisher Scientific)-labelled heterologous naïve CD4+ T cells (previously isolated with Miltenyi Naïve CD4 T cell Kit) in DCM for 5.5 days. As a positive control, T cells were cultured with anti CD3 and anti-CD28 monoclonal antibodies at 1 and 5 μg/mL respectively or media alone

as a negative control. On Day 6, T cells were analysed on a BD Fortessa flow cytometer for proliferation, measured by CellTrace Violet dilution.

Statistical analysis

Statistical analyses were performed using GraphPad Prism 9.0 and R Studio version 4. Data was assumed not to follow a normal distribution based on visual inspection or failure of normality tests. Therefore non-parametric tests were used throughout or in some cases, data was $\log_e$ transformed to approximate normality and equivalent parametric tests were applied with Bonferroni-Dunn corrections for multiple comparisons, as described in Figure legends. A GEE model was used to model the immune response as measured by cytokine levels. The model was equipped with a log-normal link function, an exchangeable correlation structure of the multiple treatments received by each donor, and adjustment for the fixed effect of age. When multiple hypotheses were adjusted for, the Bonferroni Dunn method was used. $p < 0.05$ represented statistical significance.

Study Approval

This study was approved by the Western Sydney Local Health District (WSLHD) Human Research and Ethics Committee (2019/ETH01894, 2021/ETH12256) and informed, written consent was obtained for all participants prior to the collection of tissue.

Data availability

All data are available in the main text, supplementary materials and the supporting data XLS file.

AUTHOR CONTRIBUTIONS

Conceptualization: ALC, KJS, AMD, MC, ST.

Methodology: KJS, VVS, ALC, KMB, VV, HB, JE, MC, EE, JF, FM

Investigation and data visualisation: VVS, KJS, VV, ED, DT, JE

Funding acquisition and project administration: ALC, KJS, MC

Supervision: KJS, ALC

Writing – original draft: KJS, VVS, ALC

Writing – review & editing: KJS, VVS, ALC, MC, ST, AMD

ACKNOWLEDGMENTS

We gratefully acknowledge all of the participants in this study for their critical tissue contribution that made the study possible. We thank Dr. Sara Wu, Dr. Beth Campbell, Dr. Ma Faustine Cabel and Dr. Urszula Donigiewicz for assisting with tissue samples. We also thank Dr. Harry Al-Wassiti, Monash University, Australia for the provision of research materials and Marc Lievens, GSK, Belgium for clinical supervision. Flow cytometry, histology and microscopy were performed at the Westmead Scientific Platforms, which are supported by the Westmead Research Hub, the Westmead Institute for Medical Research, the Cancer Institute New South Wales, the National Health and Medical Research Council and the Ian Potter Foundation. The authors also acknowledge the Sydney Cytometry Core Research Facility, a joint initiative of Centenary Institute and the University of Sydney, for assistance with imaging mass cytometry. This study was funded by GlaxoSmithKline Biologicals SA. V.S., E.D. and H.B. receive post-graduate scholarships from, and K.B. and A.C. are supported, by the National Health and Medical Research Council, Australia. K.S. is supported by the Peter Weiss Foundation. Shingrix and AS01 are trade marks owned by or licensed to the GSK group of companies.

612 **REFERENCES**

613 1. Cunningham AL, et al. Efficacy of the Herpes Zoster Subunit Vaccine in Adults 70 Years of Age or
614 Older. *N Engl J Med.* 2016;375(11):1019-32.
615 2. Lal H, et al. Efficacy of an adjuvanted herpes zoster subunit vaccine in older adults. *N Engl J Med.*
616 2015;372(22):2087-96.
617 3. Strezova A, et al. Long-term Protection Against Herpes Zoster by the Adjuvanted Recombinant Zoster
618 Vaccine: Interim Efficacy, Immunogenicity, and Safety Results up to 10 Years After Initial
619 Vaccination. *Open Forum Infect Dis.* 2022;9(10):ofac485.
620 4. Chlibek R, et al. Safety and immunogenicity of an AS01-adjuvanted varicella-zoster virus subunit
621 candidate vaccine against herpes zoster in adults >=50 years of age. *J Infect Dis.* 2013;208(12):1953-
622 61.
623 5. Didierlaurent AM, et al. Adjuvant system AS01: helping to overcome the challenges of modern
624 vaccines. *Expert Rev Vaccines.* 2017;16(1):55-63.
625 6. Schmader KE, et al. Impact of Reactogenicity After Two Doses of Recombinant Zoster Vaccine Upon
626 Physical Functioning and Quality of Life: An Open Phase III Trial in Older Adults. *J Gerontol A Biol*
627 *Sci Med Sci.* 2021;76(3):485-90.
628 7. Callegaro A, et al. Association Between Immunogenicity and Reactogenicity: A Post Hoc Analysis of
629 2 Phase 3 Studies With the Adjuvanted Recombinant Zoster Vaccine. *J Infect Dis.* 2022;226(11):1943-
630 8.
631 8. Didierlaurent AM, et al. Enhancement of adaptive immunity by the human vaccine adjuvant AS01
632 depends on activated dendritic cells. *J Immunol.* 2014;193(4):1920-30.
633 9. Dendouga N, et al. Cell-mediated immune responses to a varicella-zoster virus glycoprotein E vaccine
634 using both a TLR agonist and QS21 in mice. *Vaccine.* 2012;30(20):3126-35.
635 10. Detienne S, et al. Central Role of CD169(+) Lymph Node Resident Macrophages in the Adjuvanticity
636 of the QS-21 Component of AS01. *Sci Rep.* 2016;6:39475.
637 11. Coccia M, et al. Cellular and molecular synergy in AS01-adjuvanted vaccines results in an early
638 IFNgamma response promoting vaccine immunogenicity. *NPJ Vaccines.* 2017;2:25.
639 12. De Mot L, et al. Transcriptional profiles of adjuvanted hepatitis B vaccines display variable
640 interindividual homogeneity but a shared core signature. *Sci Transl Med.* 2020;12(569).

13. Grasso C, et al. Lymph node stromal cells: subsets and functions in health and disease. *Trends Immunol.* 2021;42(10):920-36.
14. Xiang M, et al. A Single-Cell Transcriptional Roadmap of the Mouse and Human Lymph Node Lymphatic Vasculature. *Front Cardiovasc Med.* 2020;7:52.
15. Papi A, et al. Respiratory Syncytial Virus Prefusion F Protein Vaccine in Older Adults. *N Engl J Med.* 2023;388(7):595-608.
16. Villadangos JA, and Young L. Antigen-presentation properties of plasmacytoid dendritic cells. *Immunity.* 2008;29(3):352-61.
17. Yu P, et al. Pyroptosis: mechanisms and diseases. *Signal Transduct Target Ther.* 2021;6(1):128.
18. Marty-Roix R, et al. Identification of QS-21 as an Inflammasome-activating Molecular Component of Saponin Adjuvants. *J Biol Chem.* 2016;291(3):1123-36.
19. Cakala-Jakimowicz M, et al. Aging-Related Cellular, Structural and Functional Changes in the Lymph Nodes: A Significant Component of Immunosenescence? An Overview. *Cells.* 2021;10(11).
20. Allen JC, et al. Understanding immunosenescence and its impact on vaccination of older adults. *Vaccine.* 2020;38(52):8264-72.
21. Panda A, et al. Age-associated decrease in TLR function in primary human dendritic cells predicts influenza vaccine response. *J Immunol.* 2010;184(5):2518-27.
22. Franceschi C, et al. Inflammaging: a new immune-metabolic viewpoint for age-related diseases. *Nat Rev Endocrinol.* 2018;14(10):576-90.
23. Ferrucci L, et al. The origins of age-related proinflammatory state. *Blood.* 2005;105(6):2294-9.
24. Gangemi S, et al. Increased circulating Interleukin-18 levels in centenarians with no signs of vascular disease: another paradox of longevity? *Exp Gerontol.* 2003;38(6):669-72.
25. Cunningham AL, et al. Advances in understanding the mechanism of action of adult vaccines. *J Clin Invest.* 2023;133(23).
26. Laing KJ, et al. Recruitment of naive CD4+ T cells by the recombinant zoster vaccine correlates with persistent immunity. *J Clin Invest.* 2023;133(23).
27. Trevaskis NL, et al. From sewer to saviour - targeting the lymphatic system to promote drug exposure and activity. *Nat Rev Drug Discov.* 2015;14(11):781-803.
28. Jin J, et al. Production, quality control, stability, and potency of cGMP-produced Plasmodium falciparum RH5.1 protein vaccine expressed in Drosophila S2 cells. *NPJ Vaccines.* 2018;3:32.

29. Louie DAP, and Liao S. Lymph Node Subcapsular Sinus Macrophages as the Frontline of Lymphatic Immune Defense. *Front Immunol.* 2019;10:347.
30. Bosteels C, et al. CCR2- and Flt3-Dependent Inflammatory Conventional Type 2 Dendritic Cells Are Necessary for the Induction of Adaptive Immunity by the Human Vaccine Adjuvant System AS01. *Front Immunol.* 2020;11:606805.
31. Skibinski G, et al. Organ culture of human lymphoid tissue. II. Marked differences in cytokine production and proliferation between slice and suspension cultures of human spleen. *J Immunol Methods.* 1997;205(2):115-25.
32. Giger B, et al. Human tonsillar tissue block cultures differ from autologous tonsillar cell suspension cultures in lymphocyte subset activation and cytokine gene expression. *J Immunol Methods.* 2004;289(1-2):179-90.
33. Belanger MC, et al. Acute Lymph Node Slices Are a Functional Model System to Study Immunity Ex vivo. *ACS Pharmacol Transl Sci.* 2021;4(1):128-42.
34. Bajenoff M, et al. Stromal cell networks regulate lymphocyte entry, migration, and territoriality in lymph nodes. *Immunity.* 2006;25(6):989-1001.
35. Qi H, et al. Spatiotemporal basis of innate and adaptive immunity in secondary lymphoid tissue. *Annu Rev Cell Dev Biol.* 2014;30:141-67.
36. Lee JKH, et al. Efficacy and effectiveness of high-dose influenza vaccine in older adults by circulating strain and antigenic match: An updated systematic review and meta-analysis. *Vaccine.* 2021;39 Suppl 1:A24-A35.
37. Streeter AJ, et al. Real-world effectiveness of pneumococcal vaccination in older adults: Cohort study using the UK Clinical Practice Research Datalink. *PLoS One.* 2022;17(10):e0275642.
38. Oxman MN, et al. A vaccine to prevent herpes zoster and postherpetic neuralgia in older adults. *N Engl J Med.* 2005;352(22):2271-84.
39. Liu BC, et al. Effectiveness of Acellular Pertussis Vaccine in Older Adults: Nested Matched Case-control Study. *Clin Infect Dis.* 2020;71(2):340-50.
40. Tseng HF, et al. Declining Effectiveness of Herpes Zoster Vaccine in Adults Aged >/=60 Years. *J Infect Dis.* 2016;213(12):1872-5.
41. Cunningham AL, et al. Immune Responses to a Recombinant Glycoprotein E Herpes Zoster Vaccine in Adults Aged 50 Years or Older. *J Infect Dis.* 2018;217(11):1750-60.

42. Agrawal A, and Gupta S. Impact of aging on dendritic cell functions in humans. *Ageing Res Rev.* 2011;10(3):336-45.
43. Jing Y, et al. Aging is associated with a numerical and functional decline in plasmacytoid dendritic cells, whereas myeloid dendritic cells are relatively unaltered in human peripheral blood. *Hum Immunol.* 2009;70(10):777-84.
44. Della Bella S, et al. Peripheral blood dendritic cells and monocytes are differently regulated in the elderly. *Clin Immunol.* 2007;122(2):220-8.
45. Willer DO, et al. Efficacy of the adjuvanted recombinant zoster vaccine (RZV) by sex, geographic region, and geographic ancestry/ethnicity: A post-hoc analysis of the ZOE-50 and ZOE-70 randomized trials. *Vaccine.* 2019;37(43):6262-7.
46. Olivieri F, et al. Antifragility and antiinflammaging: Can they play a role for a healthy longevity? *Ageing Res Rev.* 2023;84:101836.
47. Milan-Mattos JC, et al. Effects of natural aging and gender on pro-inflammatory markers. *Braz J Med Biol Res.* 2019;52(9):e8392.
48. Biagi E, et al. Through ageing, and beyond: gut microbiota and inflammatory status in seniors and centenarians. *PLoS One.* 2010;5(5):e10667.
49. Thevaranjan N, et al. Age-Associated Microbial Dysbiosis Promotes Intestinal Permeability, Systemic Inflammation, and Macrophage Dysfunction. *Cell Host Microbe.* 2017;21(4):455-66 e4.
50. Smith CL, et al. Adjuvant AS01 activates human monocytes for costimulation and systemic inflammation. *Vaccine.* 2024;42(2):229-38.
51. Day S, et al. Comparison of blood and lymph node cells after intramuscular injection with HIV envelope immunogens. *Front Immunol.* 2022;13:991509.
52. Rhodes JW, et al. Human anogenital monocyte-derived dendritic cells and langerin+cDC2 are major HIV target cells. *Nat Commun.* 2021;12(1):2147.
53. Hoffmann P, et al. Organ culture of human lymphoid tissue. I. Characteristics of the system. *J Immunol Methods.* 1995;179(1):37-49.
54. Durand M, et al. Human lymphoid organ cDC2 and macrophages play complementary roles in T follicular helper responses. *J Exp Med.* 2019;216(7):1561-81.
55. Grivel JC, and Margolis L. Use of human tissue explants to study human infectious agents. *Nat Protoc.* 2009;4(2):256-69.

56. Wagar LE, et al. Modeling human adaptive immune responses with tonsil organoids. *Nat Med.* 2021;27(1):125-35.

57. Liang F, et al. Vaccine priming is restricted to draining lymph nodes and controlled by adjuvant-mediated antigen uptake. *Sci Transl Med.* 2017;9(393).

58. Neeland MR, et al. The Lymphatic Immune Response Induced by the Adjuvant AS01: A Comparison of Intramuscular and Subcutaneous Immunization Routes. *J Immunol.* 2016;197(7):2704-14.

FIGURES

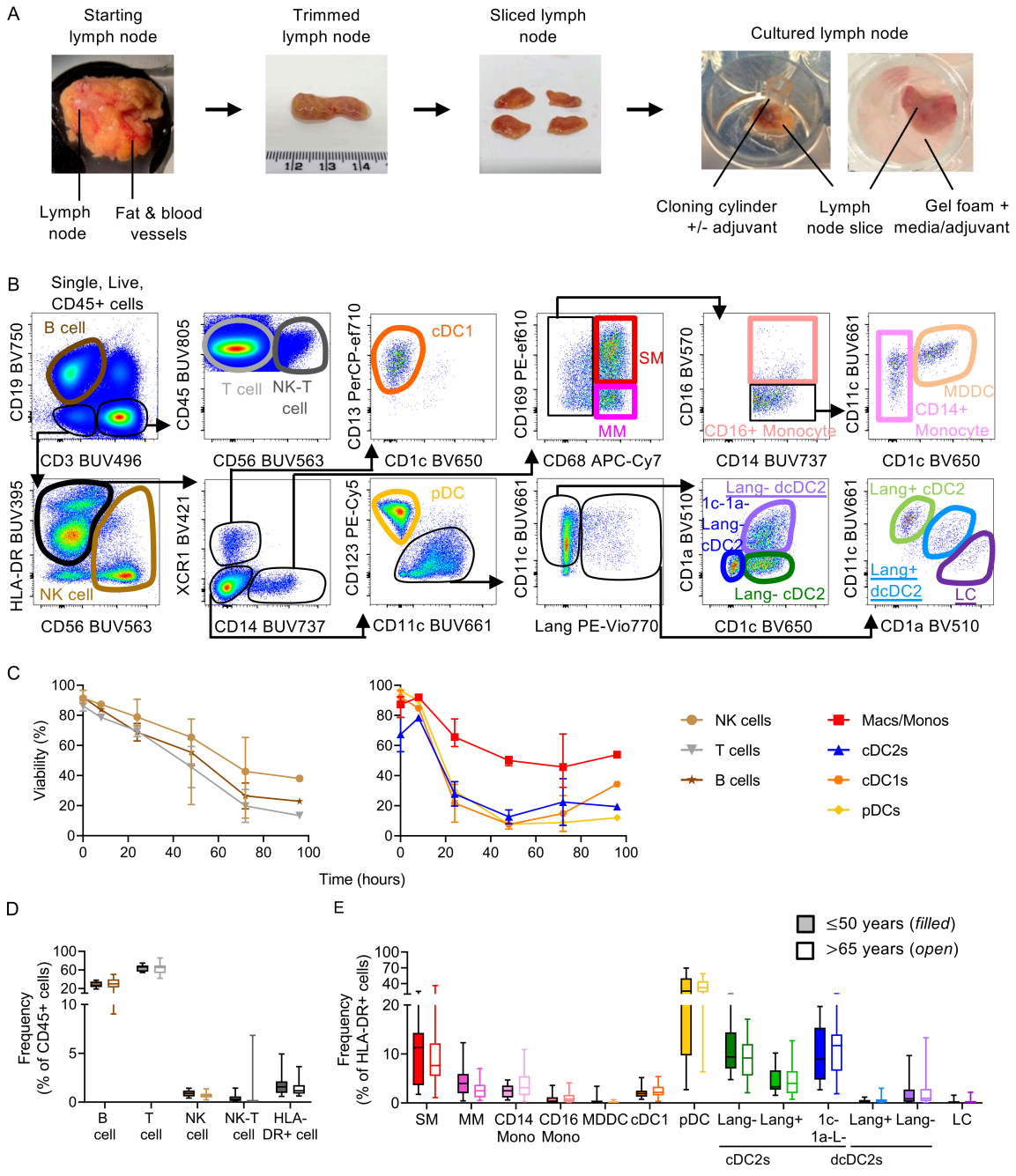

Figure 1: Human lymph node (LN) explant model for studying vaccine adjuvants in situ**.** **(A)** Fat is trimmed from human LNs which are then sliced longitudinally and placed cut face down on gel foam soaked in culture medium. For adjuvant exposure via the most physiological route (i.e., via the afferent lymph), a cloning cylinder is glued to the capsule of the lymph node and the adjuvant applied within this. For maximum cellular exposure, LN slices are bathed in

745 the adjuvant. **(B)** Flow cytometry gating strategy used to identify LN cell populations,
746 including resident and migratory (underlined) dendritic cell (DC) populations. **(C)** Viability of
747 LN lymphocyte and myeloid cell populations following in situ culture (n = 4 for 0-, 24-, 48-
748 and 72-h time points, n = 1 for 8-, and 96-h time points) was measured by flow cytometry.
749 Median with interquartile range of available donors is shown for each cell subset at each
750 timepoint. **(D)** Frequency of cell populations within fresh, uncultured LN with a comparison
751 between donors aged ≤50 years (filled boxes, n = 12) and >65 years (open boxes, n = 22).
752 Median and interquartile range are shown for lymphocyte (B, T, NK, NK-T) and myeloid
753 (HLA-DR+) cell populations as a percent of live, CD45+ immune cells and **(E)** macrophage,
754 monocyte and DC subsets within the LN as a percentage of live, CD45+, CD19-, CD3-, CD56-
755 , HLA-DR+ myeloid cells. All subset comparisons between young and old LNs were not
756 significant by Mann Whitney test using Bonferroni-Dunn correction method for multiple
757 comparisons. NK = natural killer. SM = subcapsular sinus-lining macrophage. MM =
758 medullary macrophage. Mono = monocyte. MDDC = monocyte-derived DC. cDC1/2 =
759 conventional DC type 1 or 2. dcDC2 = dermal-derived conventional DC type 2. pDC =
760 plasmacytoid DC. Lang = langerin. LC = Langerhans cells.

761

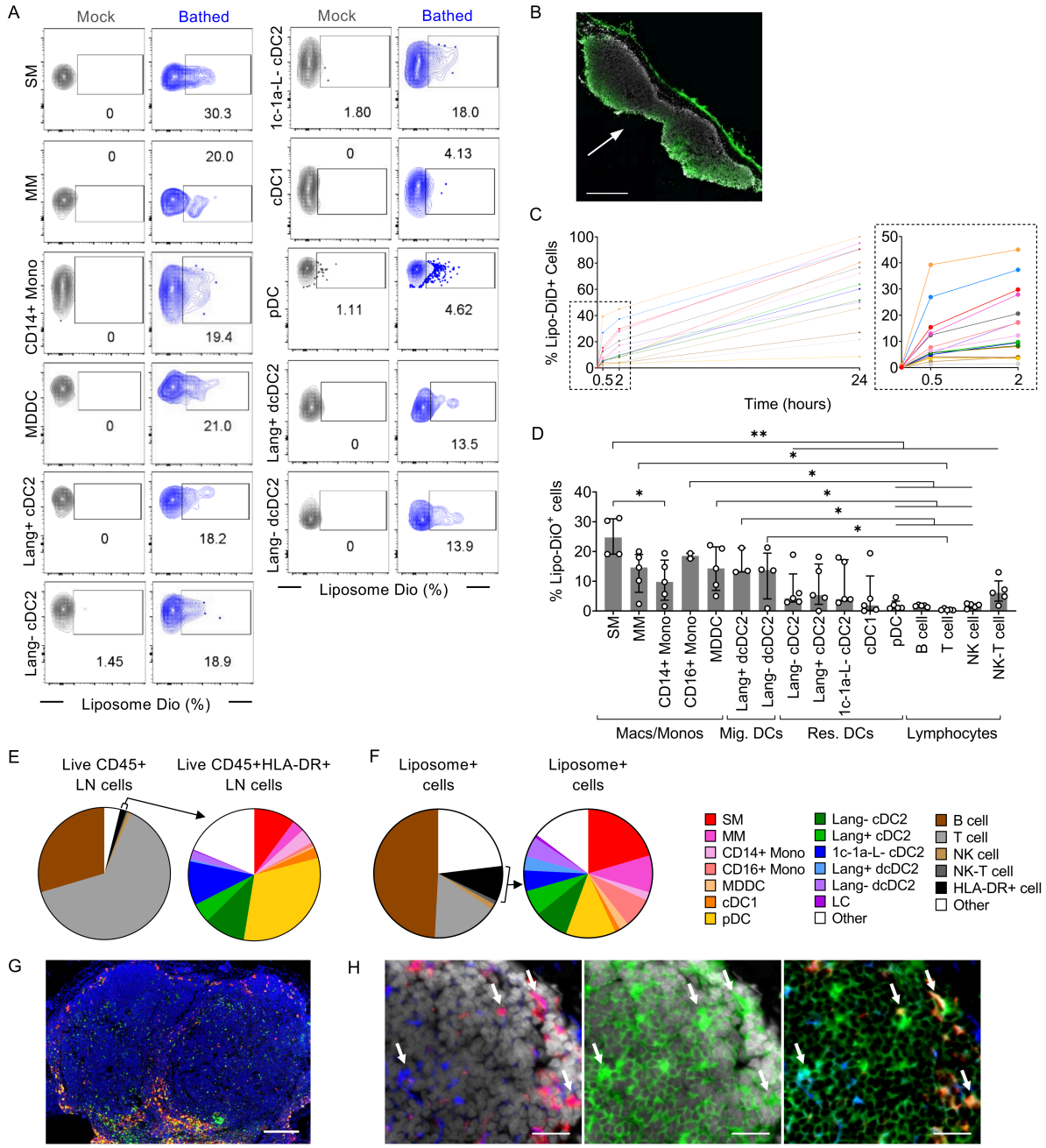

Figure 2: Fluorescent liposomes, a model for AS01, are preferentially taken up by subcapsular sinus lining macrophages in LNs. Slices of human LNs were exposed to DiO-, or DiD-labeled liposomes for 0.5, 2 or 24 h. Cells were mechanically dissociated for flow cytometry or the tissue prepared for microscopy. **(A)** Representative flow cytometry plots showing DiO-liposome uptake after 2 h bathing, by resident myeloid cells and migratory skin-derived cells (n = 3-5). **(B)** Immunofluorescence imaging of LN slice showing DiD-labelled liposomes penetrate the tissue within 30 min exposure. Arrow indicates exposed

face. Scale bar = 500μm. n = 3. **(C)** Uptake of DiD-labelled liposomes over 24 h measured by flow cytometry (n = 3). Colours in **(C)** and **(E, F)** correspond to cell subset legend. **(D)** Uptake at 2 h was compared between LN cell subsets of the major groups: Macrophages/monocytes (macs/monos), migratory dendritic cells (mig. DCs), resident dendritic cells (res. DCs) and lymphocytes. Median and interquartile range are plotted for each subset. Mixed effects analysis with Tukey's multiple comparisons test was performed. * $p < 0.05$, ** $p < 0.01$. For grouped statistical representation, the highest common p-value is presented but lower values were generated. **(E)** Immune cell subsets present in the LN (n = 50) and **(F)** making up the total liposome+ fraction after 2 h exposure (n = 5), showing cell subsets as a proportion of total live, CD45+ immune cells and myeloid cell subsets as a proportion of HLA-DR+ cells. **(G)** Imaging mass cytometry image showing CD169 (red) and CD68 (green) staining in the LN. CD169+CD68+ sinus-lining macrophages appear yellow. DAPI (blue). Scale bar = 200 μm. **(H)** CD169+ (red) subcapsular sinus macrophages and CD11c+ (blue) DCs take up DiD-labelled liposomes (green) in situ in the LN after 2 h exposure, indicated by arrows. The capsule is visible, top right. Scale bar = 25 μm.

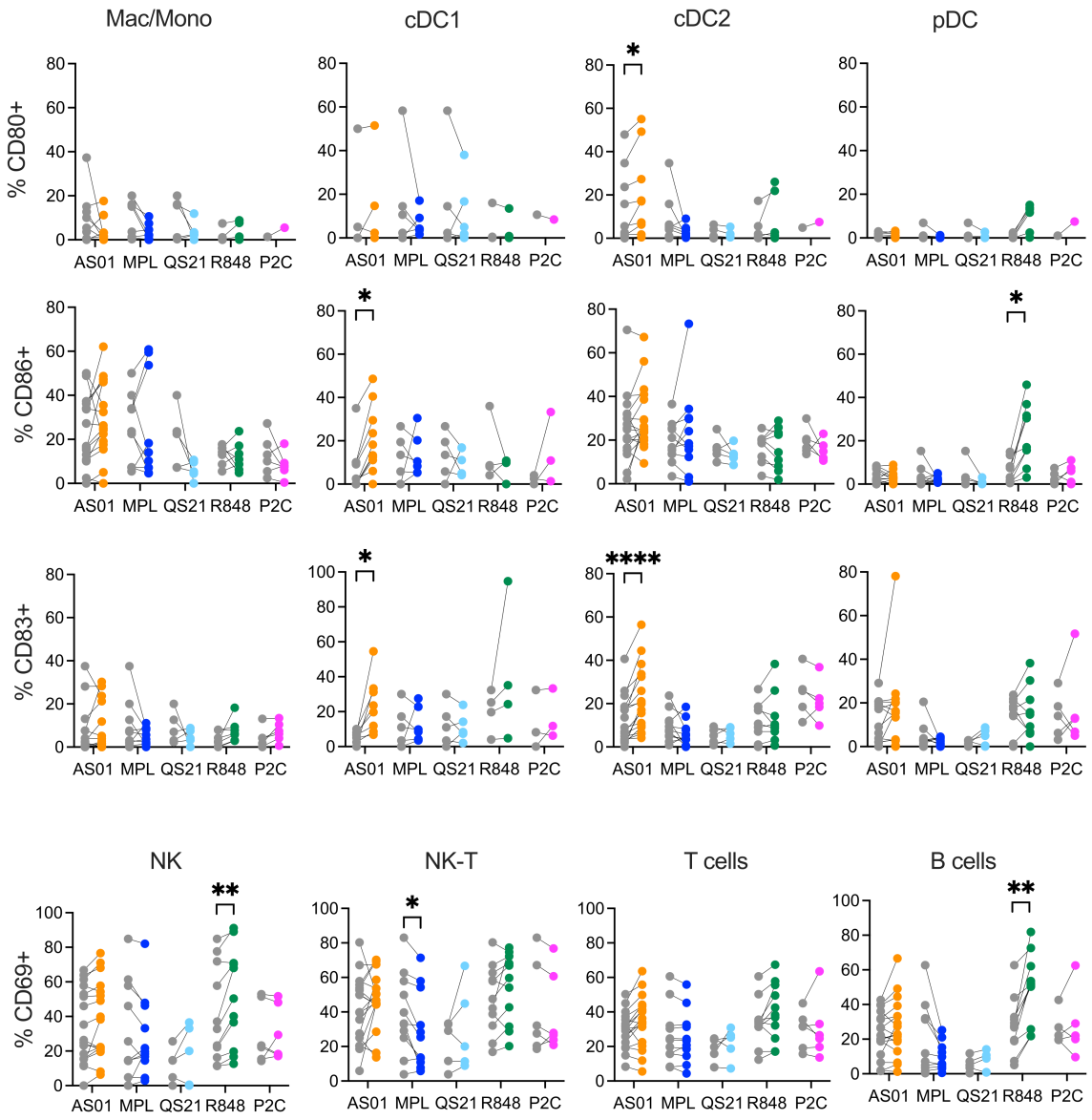

Figure 3: AS01 induces maturation of both type I and type II conventional dendritic cells in situ **in intact human LNs.** Slices of human LNs were bathed in adjuvants AS01 (orange), MPL (blue), QS-21 (light blue), R848 (green), Pam2Cys (pink, P2C) or mock treated (grey) for 24 h. Cells were then mechanically dissociated from the LN tissue and the percent of **(A)** macrophage/monocyte and dendritic cell populations expressing maturation markers CD80 (AS01 n = 3-10, MPL n = 1-4, QS-21 n = 5, R848 n = 3-6, Pam2Cys n = 1), CD83 (AS01 n = 8-17, MPL n = 1-6, QS-21 n = 5, R848 n = 4-9, Pam2Cys n = 3-6) and CD86 (AS01 n = 10-17, MPL n = 1-6, QS-21 n = 5, R848 n = 4-9, Pam2Cys n = 3-6), and **(B)** NK cells and

795 lymphocytes expressing the early activation marker CD69 (AS01 n = 17, MPL n = 6, QS-21 n
796 = 5, R848 n = 11, Pam2Cys n = 6) were assessed by flow cytometry. Wilcoxon matched-pairs
797 signed rank tests were applied with Bonferroni-Dunn correction for multiple comparisons. * p
798 < 0.05, ** p < 0.01, **** p < 0.0001.

799

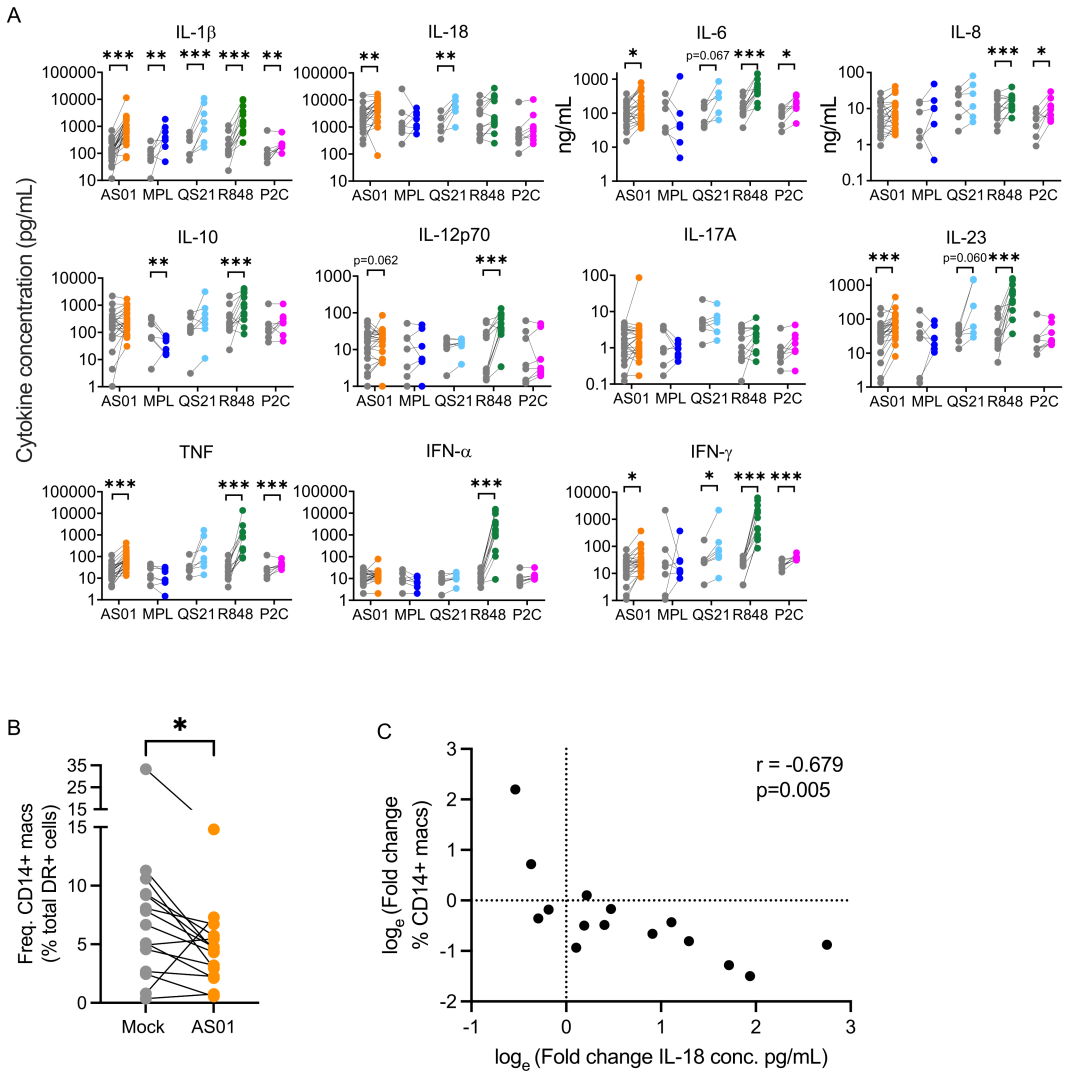

Figure 4: AS01 induces the production of pro-inflammatory cytokines in LN cells in situ**.** Slices of human LNs were bathed in adjuvants AS01 (orange, n = 27), MPL (blue, n = 8), QS-21 (light blue, n = 7), R848 (green, n = 13) or Pam2Cys (pink, n = 8) for 24 h. **(A)** Cytokine concentrations in culture supernatants were determined by LEGENDplex and compared to their donor matched mock (grey) samples. IL-6 and IL-8 were measured by ELISA. Data were $\log_e$ transformed to approximate normality and GEE models were performed with a Bonferroni correction for multiple comparisons to compare donor-paired data. * $p < 0.05$, ** $p < 0.01$, *** $p < 0.001$. **(B)** Frequency of CD14+ cells in AS01 compared to mock treated LN slices. * $p < 0.05$. **(C)** The fold-change in CD14+ cell frequency negatively correlated with the production of IL-18. Pearson's correlation was applied to $\log_e$ transformed data.

811

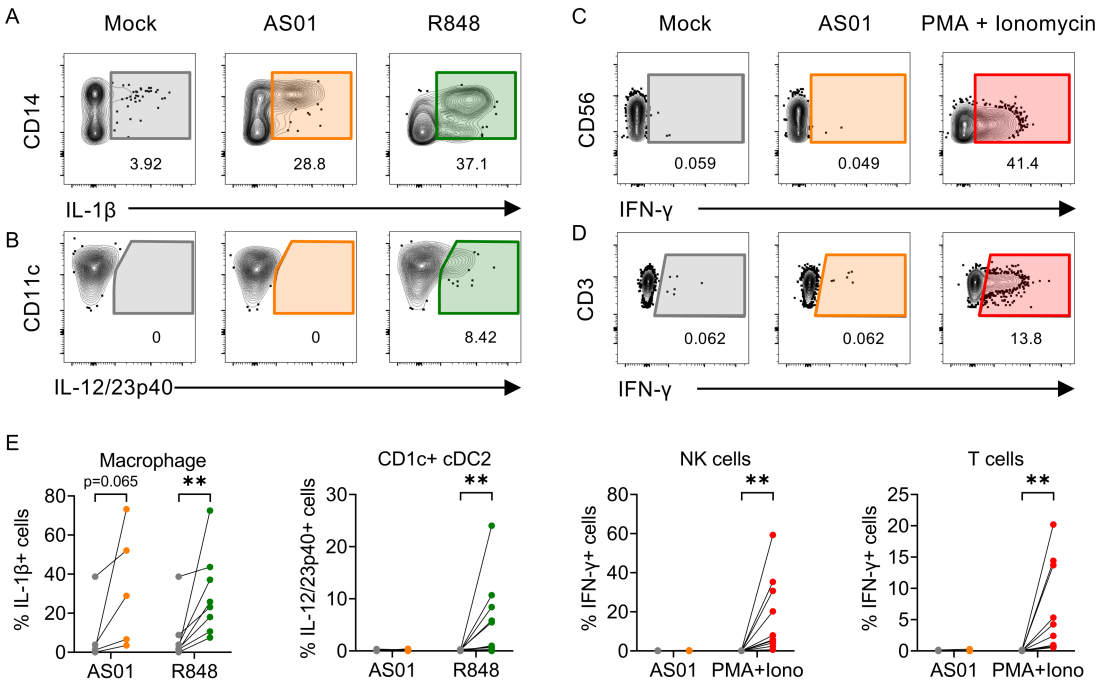

Figure 5: Macrophages produce IL-1β in response to AS01 in vitro **but downstream cytokines are not detected.** Cells were dissociated from the LN and exposed in vitro to AS01, R848 or PMA/Ionomycin for 24 h in the presence of brefeldin A. Production of IL-1β, IL-12/23p40 and IFN-γ was measured by flow cytometry. Representative data for **(A)** IL-1β and **(B)** IL-12/23p40 expression by total macrophages and CD1c+ cDC2s respectively, as well as IFN-γ expression by **(C)** NK and **(D)** T cells, in response to mock or adjuvant treatments. **(E)** Percentage of macrophages expressing IL-1β, DCs expressing IL-12/23p40 and, NK and T cells expressing IFN-γ, in response to AS01 (IL-1β n = 5, IL-12/23p40 n = 10, IFN-γ n = 13), R848 (IL-1β n = 8, IL-12/23p40 n = 12), and PMA + Ionomycin (IFN-γ n = 10). Wilcoxon matched-pairs signed rank tests were applied. ** $p < 0.01$.

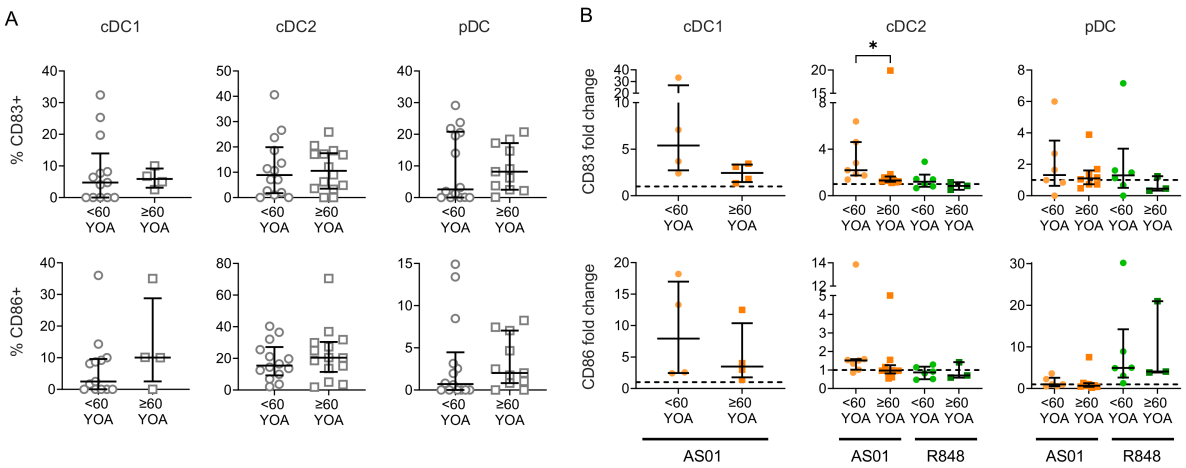

Figure 6: Expression of co-stimulatory molecules on DCs at baseline and in response to AS01 and R848 are similar between younger and older LN donors. Slices of human LNs were processed immediately (grey) and/or stimulated in situ for 24 h with AS01 (orange) or R848 (green). Cells were mechanically dissociated from the LN tissue and expression of CD83 and CD86 was assessed by flow cytometry. Comparisons were made between young (<60 YOA, circles) and old (≥60 YOA, squares) donors. **(A)** Percentage of CD83 and CD86 expression (young n = 12-14; old n = 4-14) at baseline. **(B)** Fold change in expression of CD83 and CD86 in response to AS01 (young n = 4-7; old n = 4-10) or R848 (young n = 3-6, old n = 0-3) compared to donor-matched mock samples. Not all of these samples were measured at baseline and vice versa. Medians with interquartile range are indicated throughout. Mann Whitney tests were applied for each treatment. * $p < 0.05$.

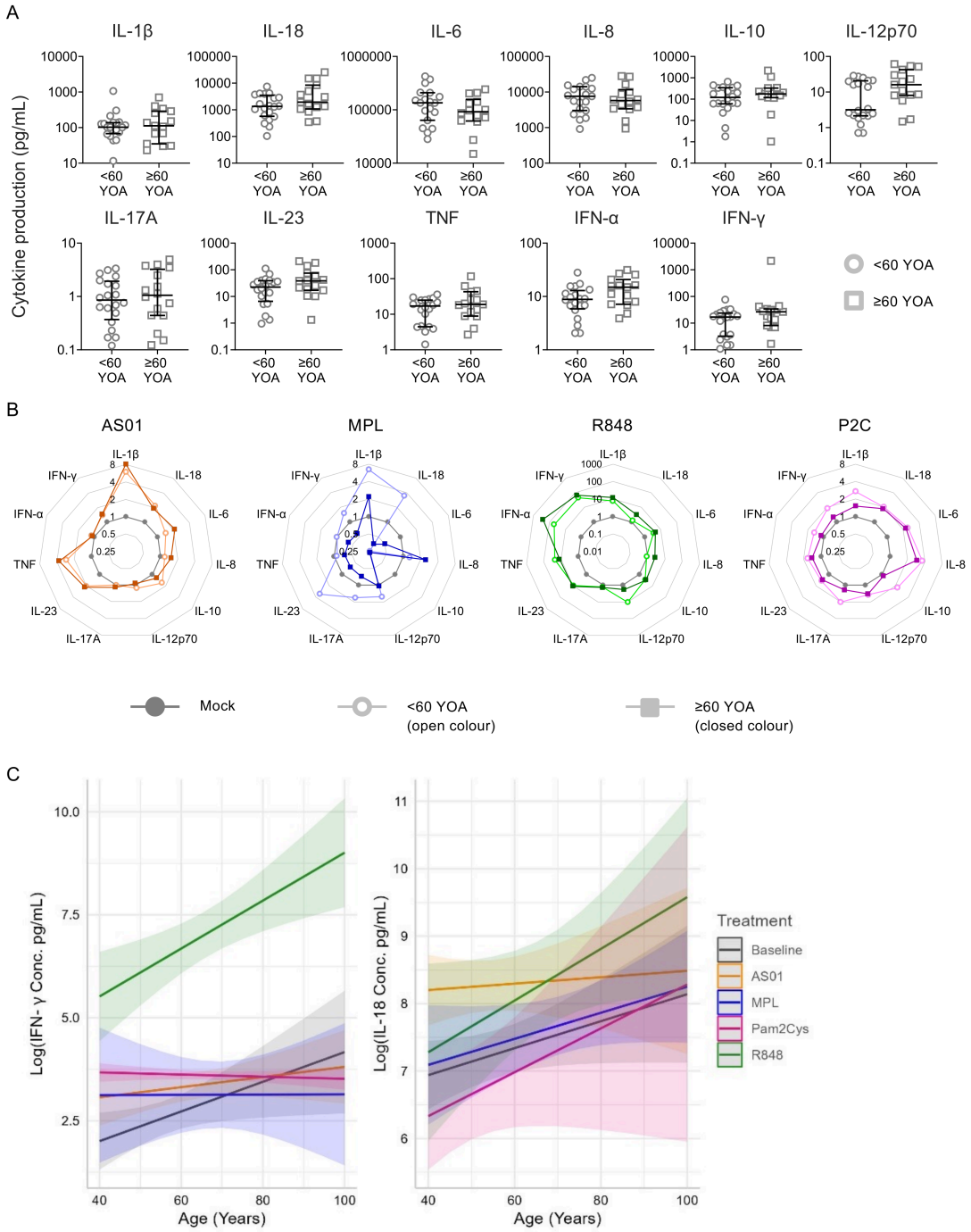

837

838 **Figure 7: The cytokine response to distinct adjuvants differs with respect to donor age.**

839 Slices of human LNs were processed immediately and/or stimulated in situ for 24 h with AS01

840 (orange), MPL (blue), R848 (green) or Pam2Cys (purple) or left unstimulated (grey) and

841 comparisons made between young (<60 YOA, circles) and old (≥60 YOA, squares) donors.

842 **(A)** Level of cytokines in unstimulated cultures (young n = 19-20=; old n = 14-15). Medians

with interquartile range are indicated. **(B)** Median fold-change in cytokine production in response to adjuvants (coloured) compared to donor-matched mock samples (grey), is plotted. AS01 (<60 n = 11, ≥60 n = 12-13), MPL (<60 n = 5, ≥60 n = 1-2), R848 (<60 n = 6-7, ≥60 n = 4), Pam2Cys (<60 n = 5, ≥60 n = 3). Mann Whitney tests corrected for multiple comparisons using the Bonferroni-Dunn method were applied. **(C)** IFN-γ and IL-18 had a significant interaction with age in a GEE model. The amount of cytokine produced in response to each adjuvant is plotted with respect to the age of the LN donor. Baseline (n = 34-36), AS01 (n = 24-25), MPL (n = 6-7), R848 (n = 12) or Pam2Cys (n = 8).

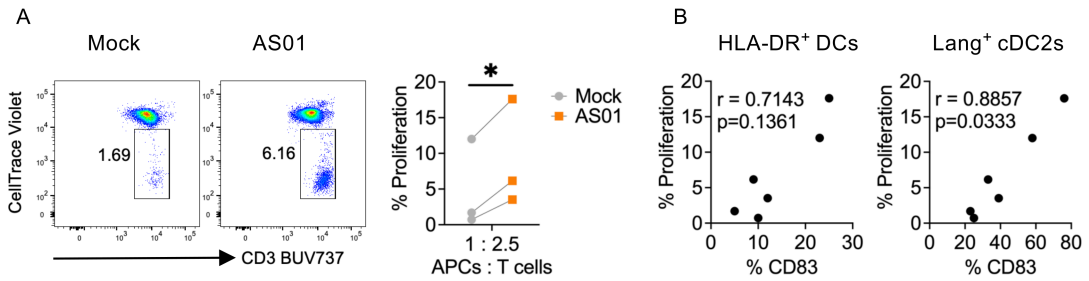

852

853 **Figure 8: Proliferation of naïve CD4+ T cells induced by AS01-exposed dendritic cells.**
854 DCs isolated from slices of human LNs that were stimulated in situ for 24 h with AS01 or mock
855 conditions were co-cultured with CellTrace Violet-labelled heterologous naïve CD4+ T cells
856 at a ratio of 1:2.5 for 5 days. **(A)** T cell proliferation was measured by CellTrace Violet dilution.
857 Student's t-test *p<0.05. **(B)** Correlation of T cell proliferation with CD83 expression on the
858 total sorted DCs and subsets from mock and AS01 treated samples was done with Spearman's
859 correlation. n=3 biological replicates.

860

Table I: Point estimates per year increase in age, derived from the GEE model, with 95% confidence intervals.

	IFN		IL-18	
Adjuvant	**Estimated Coefficient**	**95% CI**	**Estimated Coefficient**	**95% CI**
Baseline	0.027	0.014, 0.040	0.023	0.012, 0.029
AS01	0.016	0.013, 0.019	0.005	-0.007, 0.017
MPL	-0.001	-0.013, 0.011	0.019	0.018, 0.020
Pam2Cys	0.001	-0.002, 0.003	0.033	0.007, 0.058
R848	0.059	0.054, 0.065	0.038	0.036, 0.041

SUPPLEMENTAL MATERIALS

Supplemental Figure 1: Age distribution of lymph node donors.

Supplemental Figure 2: Viability of lymph node immune cells in the in situ explant model vs in vitro cultured cells.

Supplemental Figure 3: Fluorescent liposomes, a model for AS01, are preferentially taken up by subcapsular sinus macrophages following cylinder and bathing exposure in situ.

Supplemental Figure 4: AS01 does not induce maturation of macrophages and dendritic cells or activation of lymphocytes in vitro in dissociated human LN cells.

Supplemental Figure 5: AS01 induces maturation of subsets of resident type II conventional dendritic cells, only in situ at the optimal concentration.

Supplemental Figure 6: AS01 does not induce the production of key pro-inflammatory cytokines from total lymph node cells in vitro.

Supplemental Figure 7: Comparison of cytokine induction by unformulated MPL and MPL formulated in liposomes.

Supplemental Figure 8: Timecourse of LN cytokine response to adjuvants.

Supplemental Figure 9: Fold change in cytokine levels in responses to AS01 and R848 in young (< 60 YOA) and old (> 60 YOA) LN donors.

Supplemental Figure 10: FACS sort strategy and phenotype of DCs used in T cell proliferation assays.